Micromachining of Carbon Materials and Laser Micropatterning of Metal Films used as Masks for Reactive Ion Etching

Markus KUHNKE[1], Gabriel DUMITRU[2], Thomas LIPPERT[1], Enrico ORTELLI[3], Günther G. SCHERER[1] and Alexander WOKAUN[1]

[1]*General Energy Department, Paul Scherrer Institut, 5232 Villigen, Switzerland*
E-mail: thomas.lippert@psi.ch
[2]*University of Applied Sciences Aargau, 5210 Windisch, Switzerland*
[3]*Dyconex AG, 8303 Bassersdorf, Switzerland*

Microstructured carbon materials are interesting for electrochemical systems such as micro fuel cell electrodes and flow fields. Glassy carbon (Sigradur G) can be microstructured by various methods such as sawing, laser machining, and reactive ion etching (RIE). An alternative for fuel cell applications is Sigracet, a graphite in a polymer matrix. Various laser wavelengths ranging from 308 to 1064 nm can be used for the micromachining of channels in both materials, but the use of UV wavelength results in channel structures with higher aspect ratios and less debris. Compared to glassy carbon, the ablation characteristic of Sigracet is much more inhomogenous, caused by the very different properties of the two components of this material. The lack of mechanical stability limits the line density for channels in Sigracet. Reactive ion etching in oxygen plasma is not a suitable method for structuring Sigracet, as the PVDF component inhibits the etching of the carbon.

Keywords: glassy carbon, micro fuel cell, laser ablation, metal film, reactive ion etching, PVDF, Sigradur, Sigracet

1. Introduction

Fuel cells are a promising technology for energy conversion and have recently gained attention in the sector of small power supplies for portable applications such as notebooks, camcorders, and cell phones. For these applications, a miniaturized cell design was developed that reduces the number of components and simplifies manufacturing and assembly. Most alternative concepts for micro fuel cells (μFC) are based on silicon/glass technology and conventional carbon-supported platinum electrodes, but a large number of other concepts are also pursued [1].

Our approach is the fabrication of a micro fuel cell electrode in glassy carbon (GC, Sigradur®, HTW Hochtemperatur-Werkstoffe), which exhibits a high electrical conductivity and chemical inertness. The electrode consists of a channel structure with typical dimensions of 50 μm in width and a depth of ~100 μm. This flowfield provides the gas supply, a support for the electrocatalyst, and is a perfect system to study the mechanisms that determine catalyst utilization [2].

Another interesting material for fuel cells is carbon-rich PVDF (e.g. Sigracet®, SGL Carbon), which is commonly used for bipolar plates in fuel cells. In comparison to Sigradur, Sigracet is more flexible and can be easily machined by milling or compression molding, but these techniques are not suitable for the fabrication of narrow channels with high aspect ratio. Its conductivity is about one order of magnitude lower than that of GC, but sufficient for fuel cell operation. Furthermore, it is substantially less expensive (by a factor of about 20-100, depending on the size, quantity and surface quality of Sigradur).

In this paper we present various techniques for the fabrication of structures in carbon materials, focusing especially on laser machining of Sigracet and Sigradur.

2. Experimental

The carbon materials used in this investigation are Sigradur G, pyrolyzed at 2200 K from a polymer precursor, and Sigracet BMA 5, consisting of ≥ 85% of graphite in a PVDF (polyvinylidene fluoride, $-[CH_2-CF_2]-_n$) matrix. The graphitic structure of the carbon in Sigracet was determined by XRD measurements. Sigradur – like any glassy carbon – is formed of irregularly oriented graphene sheets that exhibit both sp^2 and sp^3 bonds between the layers [3]. Sigracet consists mainly of graphite and a small fraction of PVDF. Both materials provide a sufficiently low resistivity of 47 μΩm (Sigradur) and 500 μΩm (Sigracet) for fuel cell operation.

A very simple method for the fabrication of channel structures is sawing. The application of a dicing saw (ESEC, Switzerland) with a narrow saw blade allows cutting of high aspect ratio channels.

Laser ablation was performed with pulsed lasers: two excimer lasers (XeCl, 308 nm and ArF, 193 nm) and two diode-pumped Nd:YAG lasers (1064 nm and frequency tripled 355 nm). As the reflectivity of polished GC (roughness < 160 nm) is below 20% for all wavelengths in the range of 90 – 1000 nm [4], any other visible and UV wavelength should be possible to use as well. At 193 nm, the smallest reflectivity of < 1% is obtained [4].

For direct machining of GC and Sigracet, the lasers were focused onto the surface of the sample. At 355 nm a *Coherent* industrial laser system operating at 8 kHz and a pulse energy of 0.24 mJ, corresponding to a fluence of about 76 J/cm^2 in a spot area with a diameter of about 20 µm, was applied. The average pulse power was 5.7 kW at a pulse length of 42 ns. The beam was focused by a lens with f = 100 mm and scanned with a velocity of 8 - 76.8 mm/s (1 - 9.6 µm/pulse). At 1064 nm, a *Virtek Foba G10* laser system operating at 10 kHz with pulse energies of 0.62 and 0.8 mJ was used. The average pulse power was 8.3 and 10.7 kW, respectively, for a pulse length of ~75 ns. By using a focusing lens with f = 56 mm, a calculated 1/e^2 spot size of ~27 µm was achieved, resulting in a fluence of up to 140 J/cm^2. A scan velocity of 250 mm/s was used, corresponding to a pulse to pulse distance ('infeed') of 25 µm.

As an alternative method, aluminum masks for a RIE process were fabricated by laser ablation (details in [1]). Line patterns with a width of 20-60 µm were written in the Al film (400 or 600 nm thick) by imaging a round or square pinhole on the sample surface with a lens (f = 100 mm) and moving the sample with a computer controlled xyz stage while the position of the laser beam was fixed.

The ablation rates of GC and Sigracet were also determined for larger spot areas, as the ablation rates usually decrease with the high aspect ratios typical for channel fabrication. Square holes with a size of 400 µm x 400 µm were ablated into the material with an imaging setup. The average ablation depth was determined with a profilometer (Dektak 8800).

3. Results and Discussion

3.1 Sawing

In glassy carbon channel fabrication can by performed by sawing with a metal bound saw blade. Channel depths of up to 150 µm can be obtained with saw blades of 15 – 50 µm thickness. An example of a channel structure cut in glassy carbon with a 15 µm thick saw blade is shown in Figure 1. At a cut speed of 1 mm/s it takes about 20 min to fabricate a 1 cm^2 flow field of 100 channels with a length of 10 mm.

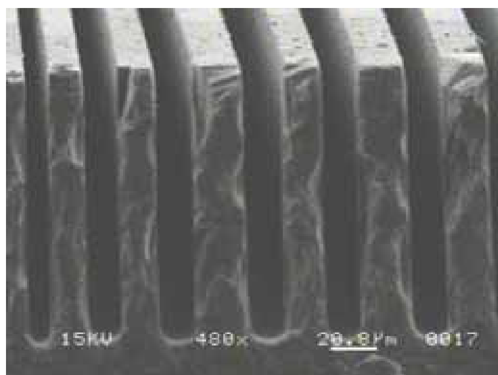

Fig. 1 SEM micrograph of channels fabricated in glassy carbon by sawing. Channel width 15 µm, depth 100 µm.

The major disadvantage of this method is the fact that only straight channels can be fabricated, as the saw can only cut the full length of the sample. This limits the geometry of the gas flow field to one design and an external gas supply and sealing is required, which is rather complex.

3.2 Laser Ablation of Carbon Materials

Glassy carbon can be ablated by lasers of various wavelengths, as demonstrated in earlier publications [1, 5]. In this paper we compare these data with the ablation rates and characteristics of Sigracet ablated by a XeCl laser (308 nm) with fluences in the range of 0.3 to 3.3 J/cm^2.

Sigracet irradiated at 308 nm exhibits inhomogeneous ablation behavior, as illustrated in Figures 2. Single shots at fluences as low as 0.3 J/cm^2 (top left image) are sufficient to modify the surface morphology and deposit debris around the ablated spot, but no significant ablation occurs. With higher pulse numbers, large features are formed in the ablated area and the amount of debris increases, but the roughness is constant ($r_a \approx 0.5 \pm 0.1$) for all pulse numbers. The depth of the structure is too low to be determined with the profilometer. The SEM pictures in Fig. 2 clearly show that the morphology in the irradiated area changes and larger structures are created in at higher fluences. For a fluence of 3.26 J/cm^{-2}, the roughness increases from $r_a = 1.4 \pm 0.5$ µm (single pulse) to $r_a = 3.9 \pm 0.3$ µm (100 pulses).

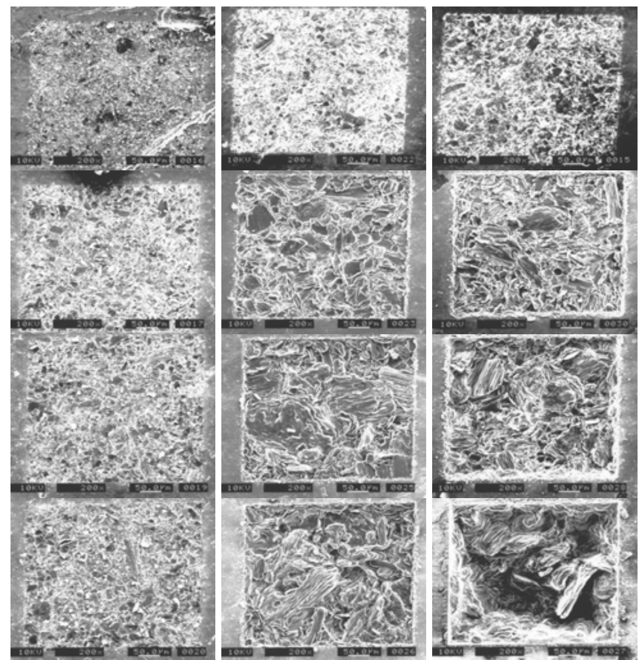

Fig. 2 Series of SEM micrographs documenting the surface modification of Sigracet by 308 nm irradiation for fluences of 0.30, 1.51 and 3.28 J/cm^2 (left to right) and 1, 31, 100 and 500 pulses (top down). Ablated area: 400 x 400 µm.

Possible explanations for the formation of these surface features may be agglomeration of PVDF, as it has a low absorption, especially at the longer wavelengths. The absorption coefficient of PVDF is about 16 cm^{-1} at 1064 nm, 46 cm^{-1} at 355 nm and 58 cm^{-1} at 308 nm [6], and therefore by more than three magnitudes below the absorption of GC, which is 143,000 cm^{-1} at 308 nm [5].

The formation of 'block'-like structures in the ablated area results in a very rough surface in the ablated region and causes problems for a reliable determination of the ablation depth. When the irradiated area is homogeneously ablated, a single line scan with a profilometer allows reasonable approximations for the ablated volume. In this case, an acceptable precision was only achieved by averaging multiple line scans. The error varies from a few percent to more than 20%, as the roughness of the pristine material is very high ($r_a = 0.7 \pm 0.2$ µm) and the irradiated area is ablated very inhomogenously. The results shown in Fig. 3 were obtained by measuring the average depth for three different line scans across the ablated crater and calculating the average.

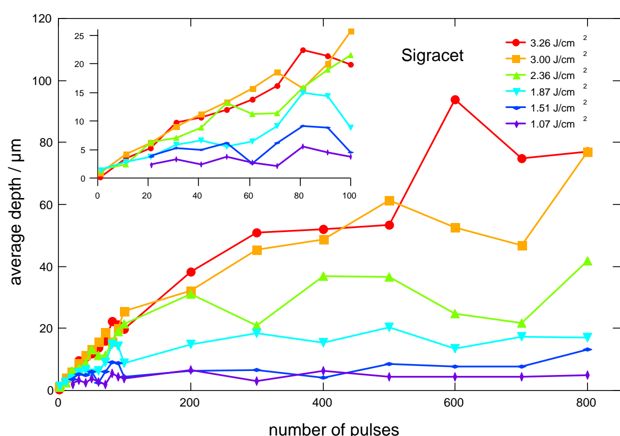

Fig. 3 Ablation depth in Sigracet for 308 nm irradiation at various fluences and pulse numbers.

The ablation depth increases roughly linearly with the number of applied pulses for up to 100 pulses (see magnification in the inset of the figure). Further irradiation results in a saturation of the crater depth, which is more pronounced for lower fluences that are still above the damage threshold of < 0.5 J/cm². This saturation is a well-known effect and can be assigned to the lowering of the effective fluence resulting from the large angle of incidence of the laser beam on the rough surface [7]. For this reason, channels of several hundred micrometers can only be achieved by using high fluences, which means that Sigracet must be machined by working in the laser focus or with an imaging setup with very high demagnification. The early saturation of ablation is in contrast to glassy carbon, which exhibits a perfectly linear increase of ablation depth with up to at least 1000 pulses.

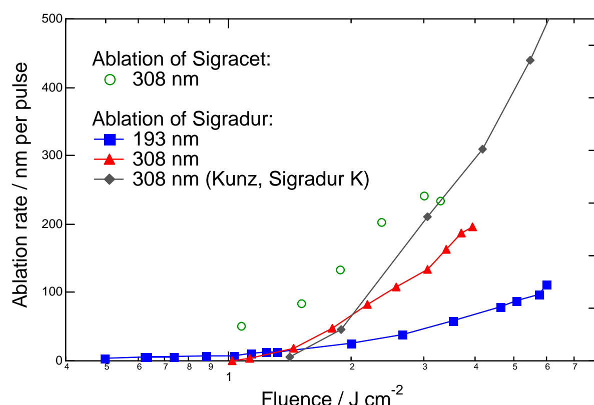

Fig. 4 Ablation rates of Sigradur and Sigracet as a function of the fluence. The errors for Sigracet are much larger than for Sigradur and may exceed 20%.

The ablation rates of Sigracet for various fluences were determined by linear fitting of the depth data obtained for ≤ 100 pulses. In Figure 4 these data are shown together with data for glassy carbon [5].

In contrast to Sigradur, Sigracet exhibits significantly higher etch rates for low fluences, which might originate from the weaker bonds between the graphene sheets of the graphite and the mixed phase material compared to the high stability of the sp^3 bonds in glassy carbon. The bond energy *within* the graphene sheets is similar to the diamond bond energy of about 7.4 eV [8, 9], but the graphitic interlayer forces are on the order of 50 meV per atom [10]. At higher fluences, the high roughness of the ablated area decreases the effective fluence and allows only deformation and possibly melting of Sigracet without significant ablation. The low absorption of agglomerated PVDF blocks can result in scattering of the incident light and further reduction of the effective fluence.

3.3 Laser Machining of Glassy Carbon

Early experiments of structuring glassy carbon were performed with a XeCl laser and an imaging setup, where a pin hole was demagnified onto the sample surface. A channel was machined by applying 20 pulses with 60 J cm^{-2} at each position with a step width of 30 µm. This method allows the fabrication of channels with a width of 50 µm and a depth of more than 200 µm, but the processing time with a 10 Hz excimer laser was by far too long [11]. For this reason, industrial Nd:YAG lasers with kHz repetition rate were used for our current experiments.

As the photon energy at 355 nm (3.49 eV) is three times larger than at 1064 nm (1.16 eV), we can expect that for the IR wavelength higher pulse energies are necessary for similar ablation rates. In addition, the reflectivity of GC is 20% at 1064 nm and only 12% at 355 nm [4]. All of those data suggest that 355 nm may yield better results.

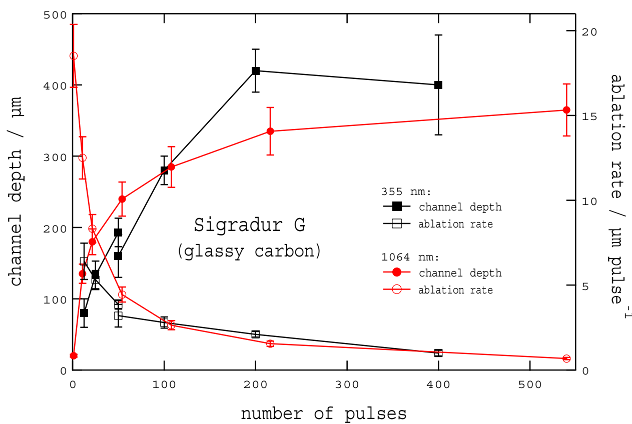

Fig. 5 Channel depth and ablation rates of GC at 355 nm (0.24 mJ) and 1064 nm (0.8 mJ) irradiation.

The ablation rates at an irradiation wavelength of 355 nm were determined by varying the infeed (1 - 4 µm/pulse) and the number of scans (1 - 16). The obtained depth was measured with a calibrated optical microscope. As the spot diameter of 25 µm leads to overlapping ablation craters, an effective number of pulses was calculated for better comparability, i.e. *number of pulses = (spot diameter / infeed) x number of scans*. The resulting ablation depths and rates are illustrated in Fig. 5.

The average ablation rate of 6.4 µm/pulse for a 80 µm deep channel decreases to ~1 µm/pulse for a 400 µm deep channel. A channel depth of 250 µm can be achieved with an average ablation rate of ~2.9 µm/pulse (infeed 2 µm, approx. 7 scans, interpolated). By increasing the infeed to 9.6 µm/pulse (7 scans), a more efficient ablation can be achieved, resulting in an ablation rate of 18 µm/pulse for a channel depth of 250 µm. As a channel depth of 250 µm is of practical interest, we will always compare the average etch rates for achieving ablation to this depth. A flow field consisting of 100 parallel channels was fabricated with an infeed of 9.6 µm/pulse, which results in V-shaped channels with a high aspect ratio. In Figure 6, a sample with 420 µm deep channels and a top width of only 45 µm is shown, but even aspect ratios > 10 are possible. No significant ablation products (‘debris’) are visible on the ridges, meaning that the carbon is removed in the form of gaseous products or very small fragments.

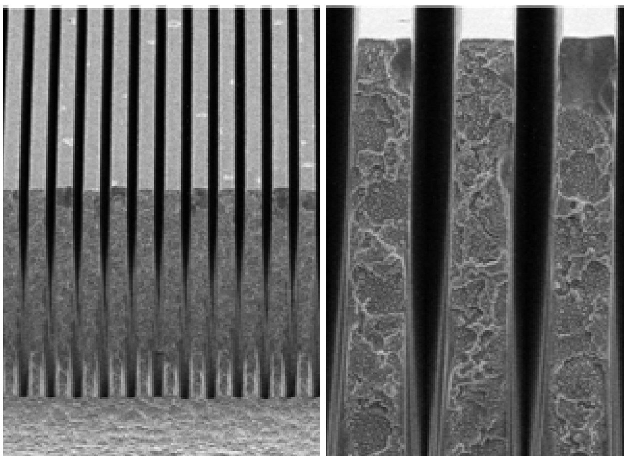

Fig. 6 Channel structure fabricated in glassy carbon with 355 nm irradiation. Pitch 100 µm, channel width ~45 µm, depth ~420 µm.

Note that all photographs of laser-machined samples are taken from channels fabricated at the sample edge. ‘Laser marks’ on the side of the sample give the appearance of much deeper channels, but precise values can only be determined by illuminating the channels and measuring the length of the bright-dark contrast.

At an irradiation wavelength of 1064 nm, similarly shaped channels can be obtained (Fig. 7), but the channel width decreases much faster towards the channel ‘bottom’, whereas in the case of 355 nm irradiation it is nearly constant in the upper half of the channel.

The initial ablation rate is higher compared to 355 nm, but decreases with increasing channel depth (Fig. 5). For a channel depth above ~280 µm the ablation rate is equal to 355 nm irradiation, despite the higher pulse energy (0.8 vs. 0.24 mJ). For the fabrication of 250 µm deep channels, an average ablation rate of ~3.8 µm/pulse can be achieved. A large amount of debris is deposited on the ridges (Fig. 8), which increases with the number of repetitive scans. For more than 50 scans, only little changes in the channel width and the amount of debris are visible. It seems that at longer wavelengths incomplete decomposition of glassy carbon occurs, possibly due to lower temperatures reached by 1064 nm irradiation.

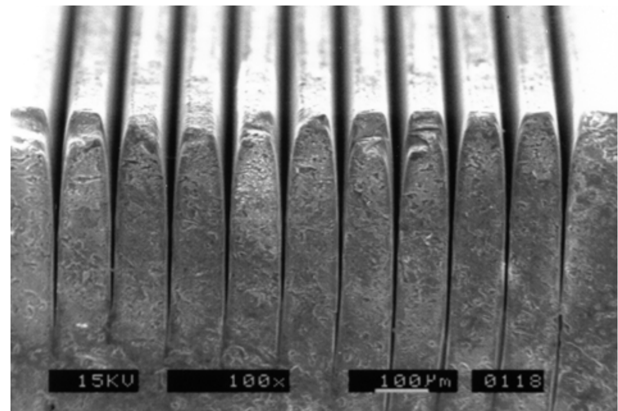

Fig. 7 Channel structure fabricated in glassy carbon with 1064 nm irradiation and 500 scans with 0.8 mJ/pulse. Pitch 100 µm, width ~55 µm, depth ~360 µm.

Even if the experiments are performed with different scan velocities and pulse energies, we can conclude that UV lasers are more suitable for the fabrication of high aspect ratio channels in glassy carbon. The ablation process at 1064 µm is less efficient than at 355 nm irradiation, as it requires higher pulse energies and produces much more debris.

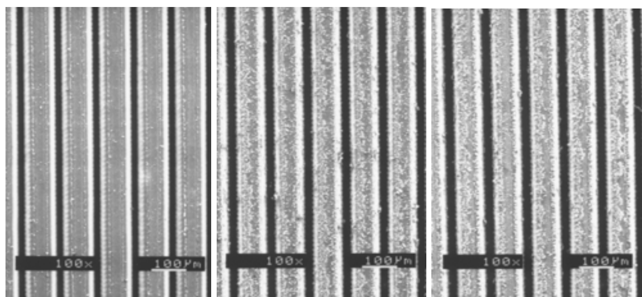

Fig. 8 Top view of channel structures fabricated in GC at 1064 nm for 10, 50 and 500 scans (left to right). The amount of debris increases with the number of pulses.

3.4 Laser Machining of Sigracet

In contrast to GC, Sigracet exhibits quite different ablation characteristics for both UV and IR wavelengths. At 1064 nm, the minimum line pitch that is possible to obtain intact structures is about 150 µm (Fig. 9, left). A line pitch of 100 µm leads to irregular damages of the ridges (Fig. 9, right), both at 0.62 and 0.8 mJ/pulse.

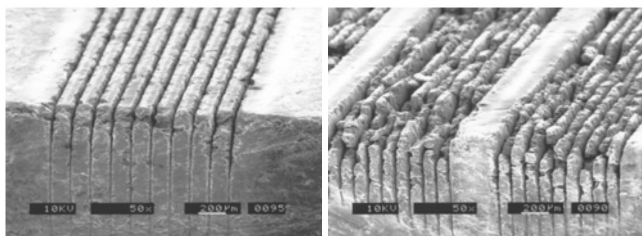

Fig. 9 Channels fabricated in Sigracet by 1064 nm irradiation. Left: 150 µm pitch, 0.8 mJ, 10 scans; Right: 100 µm pitch, 0.62 mJ, 50 and 100 scans.

A channel structure with a depth of ~180 µm and a pitch of 150 µm is shown in Fig. 10. The top width of the channel is only ~45 µm and proves that the line pitch achievable in Sigracet is not limited by the size of the ablation crater, but by the mechanical stability of the remaining ridges.

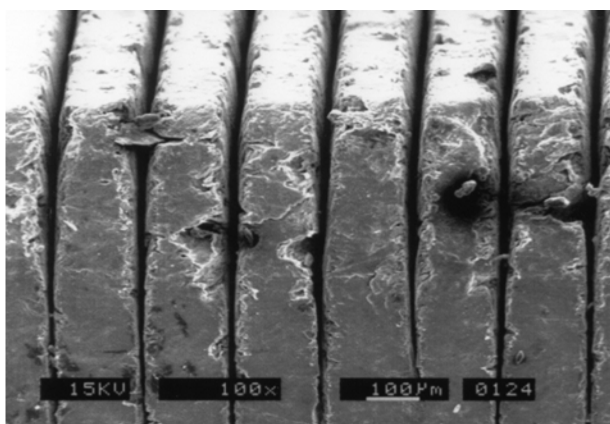

Fig. 10 Channel structure fabricated in Sigracet with 1064 nm irradiation and 100 scans with 0.62 mJ/pulse. Pitch 150 µm, width ~45 µm, depth ~180 µm.

In Figure 11, the ablation depth in Sigracet is plotted vs. the effective number of pulses. At the same pulse energy, the ablation rate for 10 pulses is equal to those achieved in glassy carbon, but 30% lower for 50 pulses, which is in contrast to the ablation rate determined for large area ablation (section 3.2). The average ablation rate for the fabrication of channels with a depth of 180 µm is about 1.7 µm/pulse. For the "reference" depth of 250 µm, we can estimate an ablation rate of << 1.5 µm/pulse, which is about one third compared to glassy carbon.

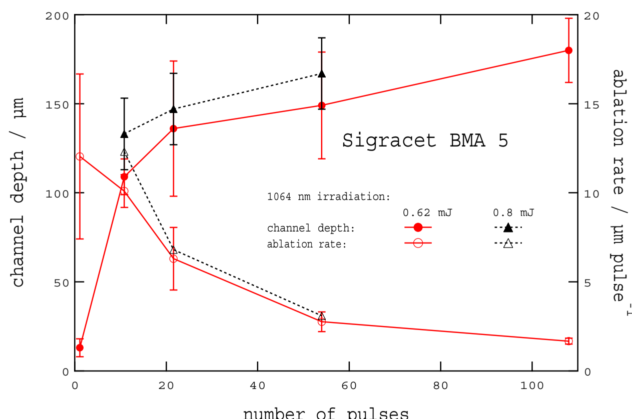

Fig. 11 Channel depths and ablation rates of Sigracet at 1064 nm.

With a focused XeCl laser beam, only channel structures with a pitch of ≥ 200 µm could be fabricated. At pitches of 100 and 150 µm the ridges crack probably due to the shock wave created by the pulse energy in the range of 0.32 to 5.24 mJ. The channels shown in Fig. 12 were fabricated with 200 pulses per position, a spot to spot distance of 50 µm and a pulse energy of 5.24 mJ. A channel depth of ~560 µm was reached at a top width of ~120 µm, corresponding to an aspect ratio of about 4.6. Even for these deep channels, an average ablation rate of 2.8 µm/pulse was achieved.

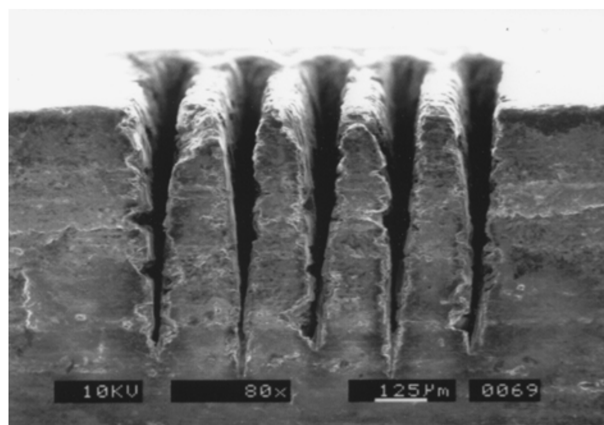

Fig. 12 Channels fabricated in Sigracet by 308 nm irradiation. Pitch 200 µm, width ~120 µm, depth ~560 µm.

It is obvious that under all tested conditions, Sigracet exhibits an ablation behavior which is much more inhomogeneous in comparison to glassy carbon. At both wavelengths, a large amount of debris is deposited around the ablated area. The channel pitches must be larger at comparable processing conditions due to the lower mechanical stability. One of the reasons for this instability is the composite material that may not provide sufficient chemical bonds between the components. Furthermore, the

graphite phase itself does not have a high mechanical stability, as it consists of separated graphite crystallites, which can be separated into the graphene sheets.

3.5 Laser Patterning of Aluminum Films

An alternative method for the fabrication of microstructures is reactive ion etching in oxygen plasma, which results in the decomposition of carbon compounds into gaseous products. For the creation of patterns, a mask has to be produced on top of the carbon material surface, which can be done by deposition of a metal layer and subsequent laser ablation of specific areas.

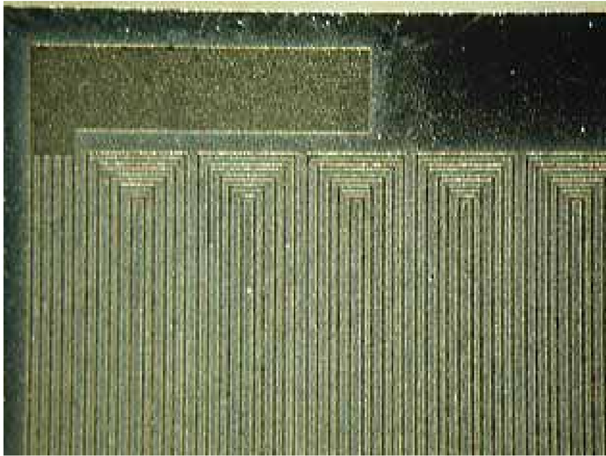

Fig. 13 Ablation of a flow field pattern in a 600 nm thick Al layer on a GC substrate (line pitch 100 µm, spot Ø 70 µm). The large 'L-shaped' area marks the region where a gas feedthrough is fabricated by electro discharge machining.

This layer is typically sputter-deposited aluminum with a thickness of 400 – 600 nm, which is structured by laser ablation at a wavelength of 308 nm, fluences of 2 – 4 J cm^{-2}, a spot size of 35 µm in diameter, a repetition rate of 20 Hz and an infeed of 10 µm/pulse. At a speed of 200 µm/s, the processing time was two hours per sample. Large amounts of debris are deposited on the sample, but the shock waves induced by the laser pulses locally clean the surface, i.e. the continuing ablation process is not affected (Fig. 13). The high flexibility and the short processing time make this method suitable for rapid prototyping.

3.6 Reactive Ion Etching of Carbon Materials

Glassy carbon can be etched in an oxygen plasma with a rate of 17 – 20 µm/h. The etching process results in well-defined channels with a trapezoid cross section and a very high bottom roughness of r_a = 2.6 µm (Fig. 14). One of the reasons for the high roughness is the micro masking caused by small Al particles remaining from the mask writing process [1].

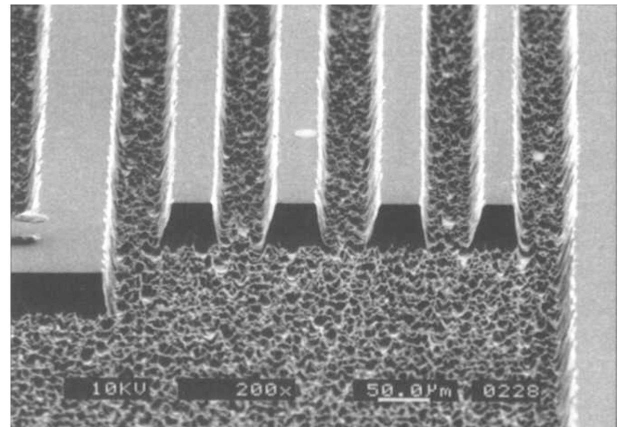

Fig. 14 Micro channels fabricated in GC by RIE (depth 52 µm).

Reactive ion etching of Sigracet was performed with the same parameters and resulted in a depth of only 10 ± 2 µm after one hour of etching. The roughness in the etched increases to $r_a \approx 2.7$ µm, which is nearly four times the original surface roughness.

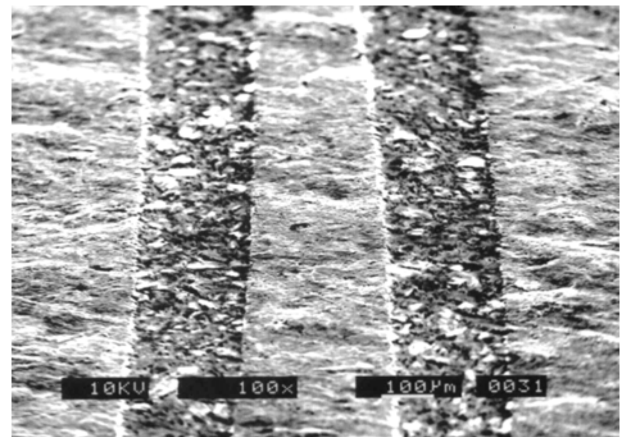

Fig. 15 Channels fabricated in Sigracet by reactive ion etching.

Both results indicate that the etching is inhibited by pronounced formation of so called "grass" in the etched area, which originates from the PVDF that is almost not etched in oxygen plasma. The formation of etch-inhibiting PTFE like films is a well-known effect for RIE processes with fluorine containing gases in carbon rich conditions [12]. For this reason, reactive ion etching in oxygen plasma is not a suitable method for structuring Sigracet.

4. Conclusions

Microstructures of high quality (aspect ratio, line density, homogeneity) can be fabricated in glassy carbon (Sigradur G) by various methods such as sawing, laser machining, and reactive ion etching (RIE). Among these techniques UV laser machining yields the highest aspect ratio and the smoothest surfaces, but the possibility of parallel processing makes RIE processes an interesting alternative. The processing characteristics of Sigracet are generally less favorable, as its two components graphite and PVDF have very different physical properties. For laser processing the low absorption of PVDF results in inhomogenous ablation and pronounced deposition of debris. The lack of mechanical stability limits the line

density for channels in Sigracet. During reactive ion etching in oxygen plasma PVDF is not etched and inhibits the etching of the graphite.

Acknowledgments

We gratefully acknowledge the contributions of Fredy Glaus for sawing of glassy carbon, Michael Horisberger for sputter coating and Alwin Frey for the XRD measurement. Finally, we thank PSI for the financial support of the project.

References

[1] M. Kuhnke, T. Lippert, G.G. Scherer, A. Wokaun, Surf. Coat. Technol., 2005. **200**: p. 730-733.
[2] U.A. Paulus, Z. Veziridis, B. Schnyder, M. Kuhnke, G.G. Scherer, A. Wokaun, J. Electroanal. Chem., 2003. **541**: p. 77-91.
[3] K. Kinoshita, *Carbon - Electrochemical and Physicochemical Properties*. 1988, New York: Wiley-Interscience. 533.
[4] L. Pajasova, L. Soukup, L. Jastrabik, D. Chvostova, Surf. Rev. Lett., 2002. **9**(1): p. 473-477.
[5] M. Kuhnke, T. Lippert, E. Ortelli, G.G. Scherer, A. Wokaun, Thin Solid Films, 2004. **453-54**: p. 36-41.
[6] E. Bormashenko, R. Pogreb, Y. Socol, M.H. Itzhaq, V. Streltsov, S. Sutovski, A. Sheshnev, Y. Bormashenko, Optical Materials, 2004. **27**(3): p. 429-434.
[7] Z. Ball, T. Feurer, D.L. Callahan, R. Sauerbrey, Applied Physics a-Materials Science & Processing, 1996. **62**(3): p. 203-211.
[8] J. Furthmuller, J. Hafner, G. Kresse, Phys. Rev. B, 1994. **50**(21): p. 15606-15622.
[9] A.K. McMahan, Phys. Rev. B, 1984. **30**(10): p. 5835-5841.
[10] R. Zacharia, H. Ulbricht, T. Hertel, Phys. Rev. B, 2004. **69**(15).
[11] J. Wei, *UV Laser Induced Microstructuring of Novel Polymers*, Dissertation in Chemistry. 2000, Swiss Federal Institute of Technology, Zürich.
[12] G. Franz, *Oberflächentechnologie mit Niederdruckplasmen*. 1994, Berlin: Springer.

(Received: April 4, 2005, Accepted: November 22, 2005)